

AFRL-RH-WP-TR-2013-0009



**In Vitro Identification of Gold Nanorods through
Hyperspectral Imaging**

**Bradley Michael Stacy
Saber M. Hussain**

**Bioeffects Division
Molecular Bioeffects Branch**

**Kristen K. Comfort
Donald A. Comfort**

**The Department of Chemical
and Materials Engineering
University of Dayton OH**



September 2012

Final Technical Report

**DESTRUCTION NOTICE – Destroy by any method that will prevent disclosure of contents
or reconstruction of this document.**

**Distribution A: Approved for
public release; distribution
unlimited. Public Affairs Case
File NO. TSRL-PA-13-0065**

**Air Force Research Laboratory
711th Human Performance Wing
Human Effectiveness Directorate
Bioeffects Division
Molecular Bioeffects Branch
Wright-Patterson AFB OH 45433**

NOTICE AND SIGNATURE PAGE

Using Government drawings, specifications, or other data included in this document for any purpose other than Government procurement does not in any way obligate the U.S. Government. The fact that the Government formulated or supplied the drawings, specifications, or other data does not license the holder or any other person or corporation; or convey any rights or permission to manufacture, use, or sell any patented invention that may relate to them.

Qualified requestors may obtain copies of this report from the Defense Technical Information Center (DTIC) (<http://www.dtic.mil>).

AFRL-RH-WP-TR-2013-0009 HAS BEEN REVIEWED AND IS APPROVED FOR PUBLICATION IN ACCORDANCE WITH ASSIGNED DISTRIBUTION STATEMENT.



David R. Mattie, Work Unit Manager
Molecular Bioeffects Branch



GARRETT D. POLHAMUS, DR-IV, DAF
Chief, Bioeffects Division
Human Effectiveness Directorate
711th Human Performance Wing
Air Force Research Laboratory

This report is published in the interest of scientific and technical information exchange and its publication does not constitute the Government's approval or disapproval of its ideas or findings.

REPORT DOCUMENTATION PAGE

Form Approved
OMB No. 0704-0188

Public reporting burden for this collection of information is estimated to average 1 hour per response, including the time for reviewing instructions, searching existing data sources, gathering and maintaining the data needed, and completing and reviewing this collection of information. Send comments regarding this burden estimate or any other aspect of this collection of information, including suggestions for reducing this burden to Department of Defense, Washington Headquarters Services, Directorate for Information Operations and Reports (0704-0188), 1215 Jefferson Davis Highway, Suite 1204, Arlington, VA 22202-4302. Respondents should be aware that notwithstanding any other provision of law, no person shall be subject to any penalty for failing to comply with a collection of information if it does not display a currently valid OMB control number. PLEASE DO NOT RETURN YOUR FORM TO THE ABOVE ADDRESS.

1. REPORT DATE (DD-MM-YYYY) 09-28-2012		2. REPORT TYPE Final TR		3. DATES COVERED (From - To) Mar 2010 – Sep 2012	
4. TITLE AND SUBTITLE In Vitro Identification of Gold Nanorods through Hyperspectral Imaging				5a. CONTRACT NUMBER	
				5b. GRANT NUMBER NA	
				5c. PROGRAM ELEMENT NUMBER 62202F	
6. AUTHOR(S) Stacy, Bradley M. ^{1,2} ; Comfort, Kristen K. ^{1,2} ; Comfort, Donald A. ² ; Hussain, Saber M. ¹				5d. PROJECT NUMBER 7184	
				5e. TASK NUMBER D4	
				5f. WORK UNIT NUMBER 7184D410	
7. PERFORMING ORGANIZATION NAME(S) AND ADDRESS(ES) ¹ 711th HPW/RHDJ, 2729 R Street, Bldg 837, Area B, WPAFB OH 45433-5707 ² Department of Chemical and Materials Engineering, University of Dayton, 300 College Park, Dayton OH 45469-0246				8. PERFORMING ORGANIZATION REPORT NUMBER	
9. SPONSORING/MONITORING AGENCY NAME(S) AND ADDRESS(ES) Air Force Materiel Command Air Force Research Laboratory 711th Human Performance Wing Human Effectiveness Directorate Bioeffects Division Molecular Bioeffects Branch Wright-Patterson AFB OH 45433-5707				10. SPONSOR/MONITOR'S ACRONYM(S) 711 HPW/RHDJ	
				11. SPONSORING/MONITORING AGENCY REPORT NUMBER AFRL-RH-WP-TR-2013-0009	
PVA12. DISTRIBUTION AVAILABILITY STATEMENT Distribution A: Approved for public release; distribution unlimited.					
13. SUPPLEMENTARY NOTES					
14. ABSTRACT Due to their unique plasmonic and optical properties, gold nanorods (GNR) have shown tremendous potential for nano-based applications extending into a variety of fields including bio-imaging, sensor development, electronics, and cancer therapy. These distinctive, shape-specific properties are strongly dependent upon the GNR aspect ratio, thus producing the ability to be targeted for an application by fine-tuning their physical parameters. It is owing to their characteristic spectral signature, which is vastly different from that of a cellular setting, that GNRs are emerging as an ideal candidate for nano-based imaging applications. However, one challenge that has emerged in the field of bio-imaging is the need to account for the observed plasmon coupling effect that arises from GNR agglomeration in a physiological environment. In this study, GNRs with aspect ratios of 2.5 and 6.0 were actively identified in an <i>in vitro</i> setting through a hyperspectral imaging (HSI) analysis; which successfully recognized and separated the light scattering pattern of these particles from that of the surrounding cells. Through inclusion of agglomerated GNR spectral patterns in the HSI spectral library, this imaging technique was able to overcome the complication of plasmon coupling, though to varying degrees. These results demonstrate the tremendous potential of GNRs coupled with HSI analysis to advance the field of nano-based sensing and imaging mechanisms.					
15. SUBJECT TERMS Nanoparticles, Gold, Synthesis, Toxicity					
16. SECURITY CLASSIFICATION OF: U			17. LIMITATION OF ABSTRACT	18. NUMBER OF PAGES 15	19a. NAME OF RESPONSIBLE PERSON S. M. Hussain
a. REPORT U	b. ABSTRACT U	c. THIS PAGE U			19b. TELEPHONE NUMBER (Include area code) NA

THIS PAGE INTENTIONALLY LEFT BLANK

TABLE OF CONTENTS

1.0 INTRODUCTION	1
2.0 EXPERIMENTAL SECTION	2
2.1 GNR Synthesis Materials.....	2
2.2 GNR Synthesis Procedure and Characterization	2
2.3 Cell Culture.....	3
2.4 GNR and Cell Preparation for Hyperspectral Imaging.....	3
2.5 Hyperspectral Imaging (HSI) System.....	3
3.0 RESULTS AND DISCUSSION.....	4
3.1 GNR Characterization and Optical Properties.....	4
3.2 GNR Agglomeration Tendencies in Culture Media	6
3.3 Employment of HSI Technology for GNR Identification	8
4.0 CONCLUSIONS.....	10
5.0 REFERENCES	12
6.0 LIST OF ABBREVIATIONS.....	15

LIST OF FIGURES

Figure 1: TEM Images of Synthesized Gold Nanorods.....	4
Figure 2: Spectral Profiles of Gold Nanorods and HSI Sensing Capabilities.....	5
Figure 3: Gold Nanorod Agglomeration Patterns Assessed through Darkfield Imaging.	6
Figure 4: Gold Nanorod Spectral Plots.....	8
Figure 5: In Vitro Identification of Gold Nanorods.....	9
Figure 6: Summary of HSI Technology and Work Performed.....	11

1.0 INTRODUCTION

Currently, gold nanorods (GNRs) are being widely researched for utilization in consumer, military, and medical based applications, including bioimaging, catalysis, sensor development, and photothermal therapy [1-3]. What makes GNRs particularly attractive for these nano-based mechanisms are their general biocompatibility, unique plasmonic properties, and spectral signature spanning both the visible and near infrared (NIR) regions [4,5]. In particular, the distinct optical properties associated with GNRs are advantageous for imaging and sensing applications [6,7].

Owing to their plasmonic properties, GNRs scatter light at the same frequency with which it absorbs. This is an extremely useful tool for the prediction and implementation of particle light scattering as an actuator. This plasmon resonance is generated by photon activation of electrons on the nanoparticle surface inducing a uniform oscillation [8,9]. A hallmark of GNR optical properties is that they exhibit two surface plasmon resonance peaks; the transverse and the longitudinal corresponding to the radial and length dimensions, respectively [10]. Another advantage of GNRs is that their distinct optical properties are tunable, with the longitudinal peak shifting further into the NIR spectrum with increasing aspect ratio (AR) [11,12]. However, when GNRs are in close proximity to one another, a plasmon coupling effect occurs which can influence the dependent spectral properties of the particles, adding a layer of complexity to their identification in a cellular environment [13]. Therefore to successfully implement GNRs into sensing and imaging applications, it is critical to evaluate and account for this environment-dependent modification of their spectral signatures.

One technique that has recently emerged to track and identify materials or objects through their light scattering spectra is Hyperspectral imaging (HSI). HSI analysis combines the use of high resolution microscopy and real time spectroscopy for the precise measurement of a spectral profile at individual pixels within a micrograph. Using darkfield microscopy, an HSI system has the ability to record and track the spectrum of metallic nanoparticles [14-16]. The HSI system reads the spectra of an object of interest and stores that information into a library. Once an image is taken, an area is scanned and cross-referenced through the collected library to generate a match. If an identical spectral profile is found, the HSI system then actively classifies and tags that pixel. Therefore while traditional techniques, such as dark field imaging, can capture GNR location, HSI is also able to separate and identify these particles from their surroundings.

Even though HSI technology is in its infancy, it has demonstrated tremendous potential to enhance the areas of nanoparticle scanning, imaging, and sensing. One area under current investigation is the employment of HSI as a technique for characterizing metallic nanoparticle agglomeration patterns and identification of intracellular particle fate [17-19]. As the light absorbance of tissue is dramatically different from that of a plasmonic particle [20], HSI offers a unique mechanism for the *in vitro* identification and tracking of target nanoparticles following

introduction into a biological system. We sought to further explore the capabilities of the HSI system by testing if it could actively identify GNRs, which due to their dual surface plasmon resonance peaks are more complex particles. As such, the goal of this study was to selectively and efficiently detect GNRs within an *in vitro* model through an HSI analysis. As the spectral signature of GNRs is highly dependent upon AR, this investigation included both shorter (AR 2.5) and longer (AR 6.0) nanorods to validate this method of GNR identification. Even with a spectral shift caused by biological media, our results demonstrated successful recognition of both GNR sets and identified that the transverse peak may be optimal for GNR sensing applications. Furthermore, this study demonstrated the capability and plausibility of this advanced imaging technology for future utilization.

2.0 EXPERIMENTAL SECTION

2.1 GNR Synthesis Materials

The cetyltrimethylammonium bromide (CTAB-98%) was obtained from GFS chemicals (Powell, OH, USA). The chloroauric acid (99.9%), ascorbic acid (99.5%), silver nitrate (99.9%), sodium borohydride (99.9%), and tannic acid (98%) were purchased from Sigma Aldrich (St.Louis, MO, USA). The benzyldimethylammonium chloride (BDAC-98%) was obtained from TSI Incorporated (Shoreview, MN, USA). It is important to note the source of the chemicals can have a significant effect on the synthesis and functionalization process. Furthermore, high grade reagents are critical for the reproducible and uniform synthesis of GNRs.

2.2 GNR Synthesis Procedure and Characterization

The GNRs were synthesized using a dual surfactant-wet chemistry based process with CTAB and BDAC as previously demonstrated [21,22]. Briefly, this optimized procedure utilized a seed solution (0.1M CTAB and 0.1M chloroauric acid) and a growth solution (0.1 M CTAB, 0.1 M silver nitrate, 0.1 M chloroauric acid, and BDAC). The gold salt in the seed solution was reduced by the addition of ice cold sodium borohydride (0.1M) and rapidly stirred at room temperature for five minutes. To tune the GNR aspect ratio, different concentrations of BDAC were used in the growth solution (0-0.15 M). To the growth solution, 0.1 M ascorbic acid and the five minute old seed solution was added and stirred at room temperature for 24 hours to ensure complete reaction. The GNRs were then purified through a combination of centrifugation and depletion-induced separation and functionalized with tannic acid to reduce cytotoxicity and promote cellular uptake [23]. To verify successful coating with tannic acid and removal of the particle-bound CTAB, a surface charge analysis was performed on a Malvern Zetasizer (Worcestershire, UK). To confirm particle morphology and size, transmission electron microscopy (TEM) imaging was completed on a Hitachi H-7600 (Tokyo, Japan). Actual size

measurements of the gold nanorods were performed using ImageJ (National Institute of Health; Bethesda, MD, USA) software, and included the counting of over 100 particles per aspect ratio. To visualize the unique optical properties of the synthesized GNRs, UV-VIS analysis was carried out using a Varian Cary 3000X (Palo Alto, CA, USA).

2.3 Cell Culture

The human lung epithelial cell line, A549, was utilized in this study and purchased from ATCC (Manassas, VA, USA). The cells were maintained in RPMI 1640 media supplemented with 10% fetal bovine (ATCC) serum and 1% penicillin/streptomycin (ATCC) and incubated at 37 °C and 5% carbon dioxide. Prior to experimentation, cells were sub-cultured in 10 cm petri dishes and grown to 80% confluence.

2.4 GNR and Cell Preparation for Hyperspectral Imaging

For HSI spectral analysis of GNRs alone in media, the particles were diluted to a concentration of 50 µg/ml and mixed well. Next, 20 µl was placed onto a silanized microscope slide and incubated for 10 seconds at room temperature to allow for attachment. The excess solution was then removed and the slides were sealed for imaging and spectral analysis.

For cell preparation, A549 cells were seeded at a concentration of 2×10^5 cells per chambered microscope slide (Fisher Scientific; Pittsburgh, PA, USA) and incubated at 37°C. The following day, the cells were then dosed with 15 µg/ml GNRs and returned to the incubator for an additional 24 hours. The GNR exposed cells were then washed to remove unbound GNRs and fixed with 4% paraformaldehyde. The chambered walls were then removed and 20 µl of culture media was added to the slide, and the slide was sealed for imaging.

2.5 Hyperspectral Imaging (HSI) System

The HSI system employed in this study was a CytoViva system that combines an ultra high power fluorescence microscope, with a darkfield condenser, visible near infrared (VNIR) real-time hyperspectral imager, imaging camera, and an integrated software analysis system. This system allowed for the overlay of darkfield and fluorescent images using a combination of halogen and mercury light sources. The HSI images and resultant spectral data were collected and analyzed using ENVI software (Exelis Visual Information Systems, Boulder, CO).

3.0 RESULTS AND DISCUSSION

3.1 GNR Characterization and Optical Properties

To evaluate the potential of particle tracking *in vitro*, GNRs with aspect ratios (AR) of 2.5 and 6.0 were synthesized for this study. These GNRs were then functionalized with tannic acid, which was specifically chosen to improve the degree of cellular uptake. For this analysis having a higher internalized concentration of GNRs was advantageous as the purpose was to track and identify intracellular nanomaterials. Following purification, the GNRs were visualized with TEM to verify rod-shaped morphology and evaluate size uniformity (Fig. 1). Through quantitative measuring and analysis it was determined that GNR AR 2.5 and 6.0 have actual aspect ratios of 2.55 ± 0.27 and 6.02 ± 0.55 , respectively.

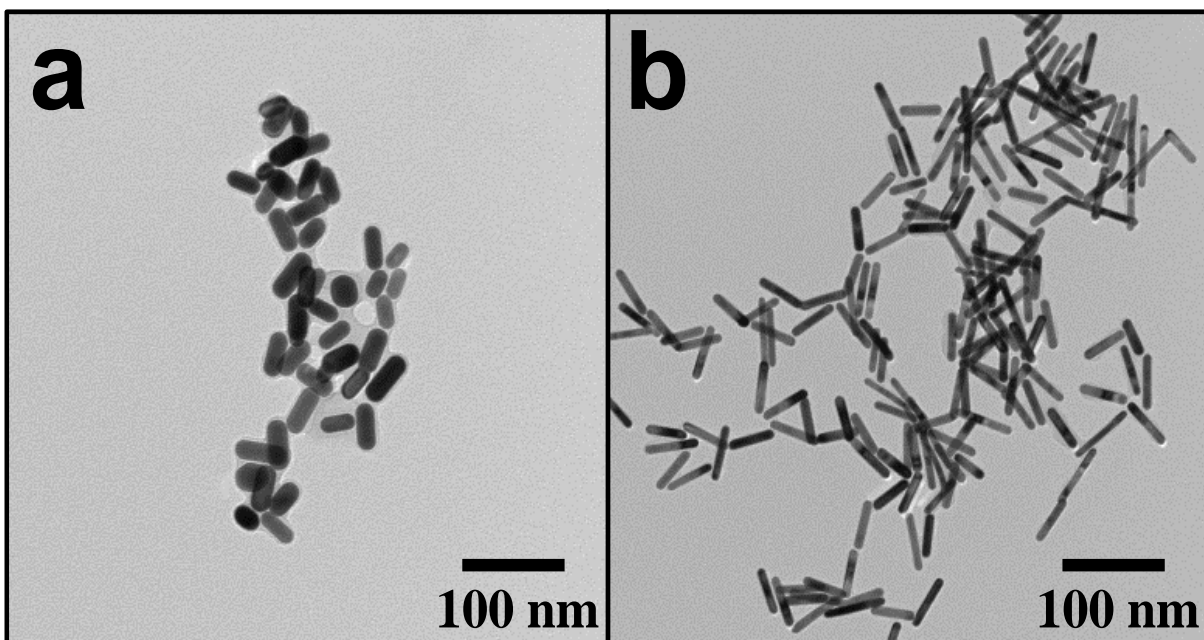


Fig. 1 TEM Images of Synthesized Gold Nanorods. Representative TEM images of tannic acid functionalized GNRs of (a) AR 2.5 and (b) AR 6.0 were used to verify particle morphology and size distribution.

The dependence of nanorod optical properties on AR is well defined; with the longitudinal peak known to shift further into the NIR spectrum with increasing AR [24]. The two GNRs employed in this investigation were purposely selected due to their unique spectral signatures, as a substantial difference in their longitudinal wavelengths was anticipated. To verify, UV-VIS analysis was performed (Fig. 2a) and it was found that the resonance peak of the longitudinal band appeared at 655 nm for AR 2.5 and 1019 for AR 6.0, a separation of 364 nm. With the presence of two plasmonic peaks, the question also arose if utilizing the transverse or the longitudinal peak would be optimal for emerging HSI technology. As the HSI camera is only capable of accurately sensing between approximately 500 and 700 nm (Fig. 2b), it facilitated this investigative question through a forced selectivity. For AR 6.0 the longitudinal peak is located at 1019 nm, well out of the camera sensitivity. As such, the transverse peak ($\lambda=525\text{nm}$) was the targeted spectral range for this GNR set. The longitudinal peak of AR 2.5 occurs at 655 nm, well within the HSI camera specifications, permitted for targeting of its longitudinal plasmonic band. Therefore, this set-up simultaneously allowed for the evaluation of two different GNR sets with ARs 2.5 and 6.0 being detected through their longitudinal and transverse peaks, respectively.

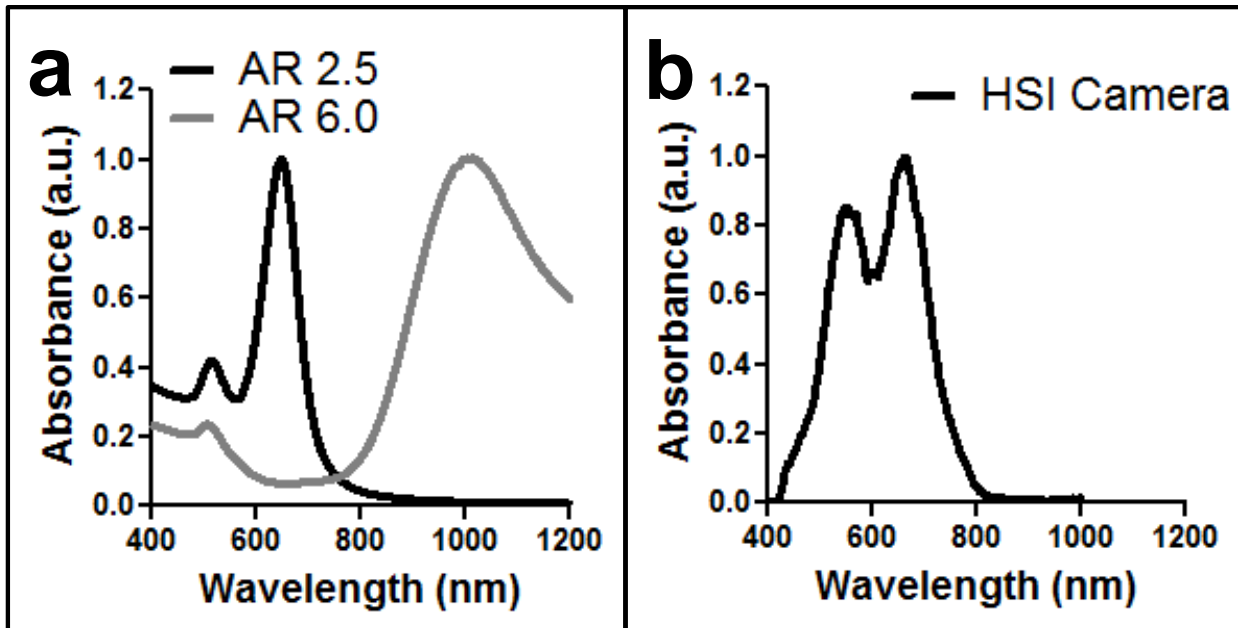


Fig. 2 Spectral Profiles of Gold Nanorods and HSI Sensing Capabilities. **a** UV-VIS analysis was performed to identify the spectral signature of the GNR sets. **b** The detection camera associated with the HSI system displays a finite sensing capabilities, which limits sensing in part of the NIR range.

3.2 GNR Agglomeration Tendencies in Culture Media

It has been previously established that when dispersed in cell culture media, the ionic strength, refractive index, and protein concentration directly impacts the optical properties, agglomeration state, and stability of nanomaterials [24, 25]. Generally, as growth media has an increased ionic strength over water, it induces significant particle aggregation following dispersion. As a result, increased plasmon coupling occurs leading to a disruption in the spectral signature; all occurring from an alteration of fluid composition. Therefore it is crucial to indentify to what degree the GNRs agglomerated in culture media and obtain a series of spectral profiles to input into the HSI system for recognition. To accomplish this task, GNRs were exposed to cellular growth media and the extent of GNR aggregation was visualized using darkfield microscopy (Fig. 3). As expected, the presence of large GNR agglomerates was easily identified for both ARs, though the presence of some individual particles was also observed. This considerable modification to GNR distribution suggests a high potential for the occurrence of a plasmon shift brought on by particle agglomeration *in vitro*.

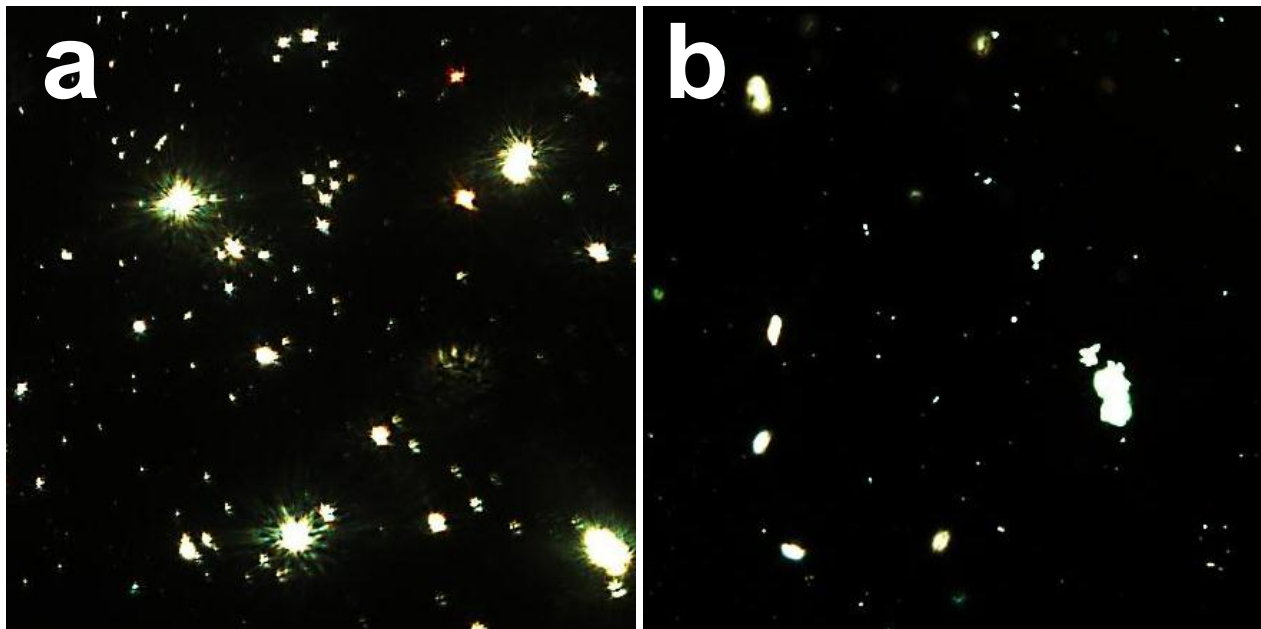


Fig. 3 Gold Nanorod Agglomeration Patterns Assessed through Darkfield Imaging. High resolution, darkfield microscopy images were taken to qualitatively evaluate the extent of GNR agglomeration of (a) AR 2.5 and (b) AR 6.0. The spectral signatures of these particles were collected and included in the spectral library of the HSI system for later identification.

To validate this hypothesis, from this darkfield analysis spectral data was collected for both individual particles and agglomerates for comparison and GNR tracking purposes. The reason for this is that any noted shift in the GNR spectral signature needs to be accounted for to successfully aid in the identification of GNRs internalized by the A549 cells. A number of representative spectral profiles were obtained and are shown in Figure 4 for AR 2.5 (Fig. 4a) and AR 6.0 (Fig. 4b). These spectral plots are a collection of representative light scattering readings taken from the GNRs; plotted on an arbitrary y-axis so they could be vertically spaced to show multiple readings simultaneously. For AR 2.5, as expected, two peaks are clearly visible which are indicative of both the transverse and longitudinal nanorod dimensions, as previously seen with the UV-VIS data. However, when directly compared to the UV-VIS result, a clear alteration in the spectra was detected with a noticeable shift to the left. This modification is easily explained by the extensive GNR agglomeration detected in the darkfield imaging, which changes the way that light photons perceive the particles. When examining AR 6.0 GNRs, even though extensive agglomeration was visible, only a minimal shift in the spectra was detected; approximately 5 nm from 525 to 520 nm. This is due to the fact that the longitudinal peak lies outside the measurable range of the HSI system, and therefore the transverse peak was used for detection. It has been previously seen, that the transverse spectral peak is not as susceptible to aggregation-induced shifts as the longitudinal peak [26,27], and that trend was verified in this study.

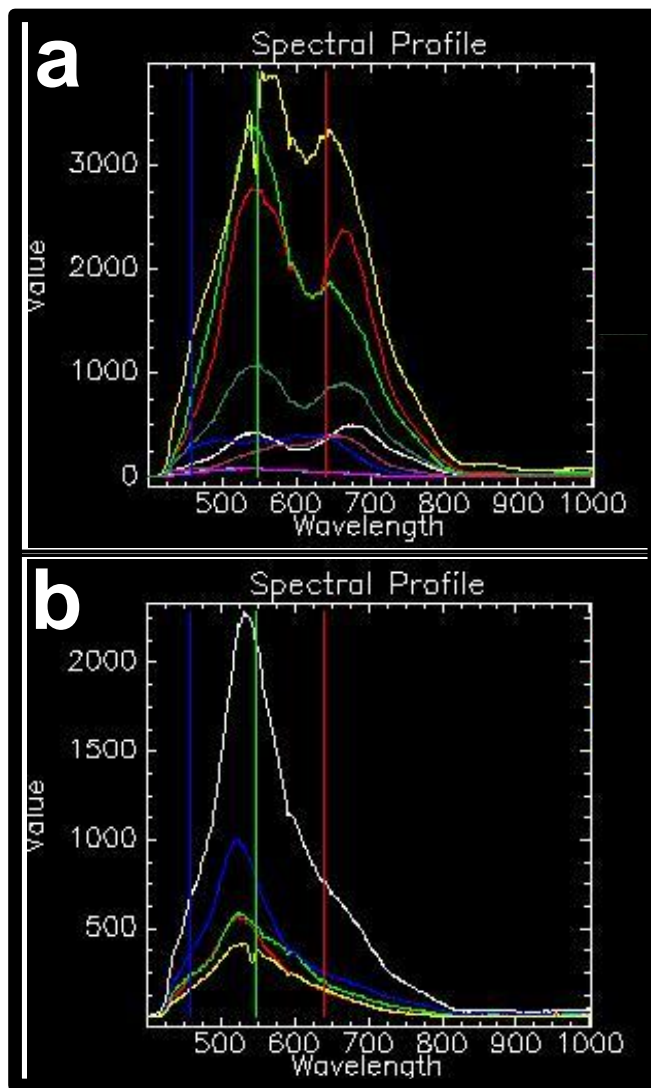


Fig. 4 Gold Nanorod Spectral Plots. Representative spectral plots (arbitrary units) obtained from tannic acid functionalized GNRs of (a) AR 2.5 and (b) AR 6.0 following dispersion in growth media. Numerous light scattering profiles are shown on each figure section for comparison with the vertical lines placed to aid in evaluating plasmon band shifts.

3.3 Employment of HSI Technology for GNR Identification

Next, using this collected GNR spectral data, the HSI system was employed to locate either AR 2.5 or AR 6.0 in A549 cells, a human lung epithelial line. As shown in Figure 5, both sets of GNRs were successfully identified *in vitro* through their spectral signature alone. The HSI system uses a red tag as a means of marking identified particles, as shown in the zoomed in

images (Figs. 5b and 5d). This was accomplished by cross-referencing the previously obtained spectral signature of the GNRs (Fig. 4) with the scanned profiles of the GNR dosed A549 cells, and highlighting the matches. While both particles were effectively recognized with the cell system, the efficiency of this process was varied between the two samples.

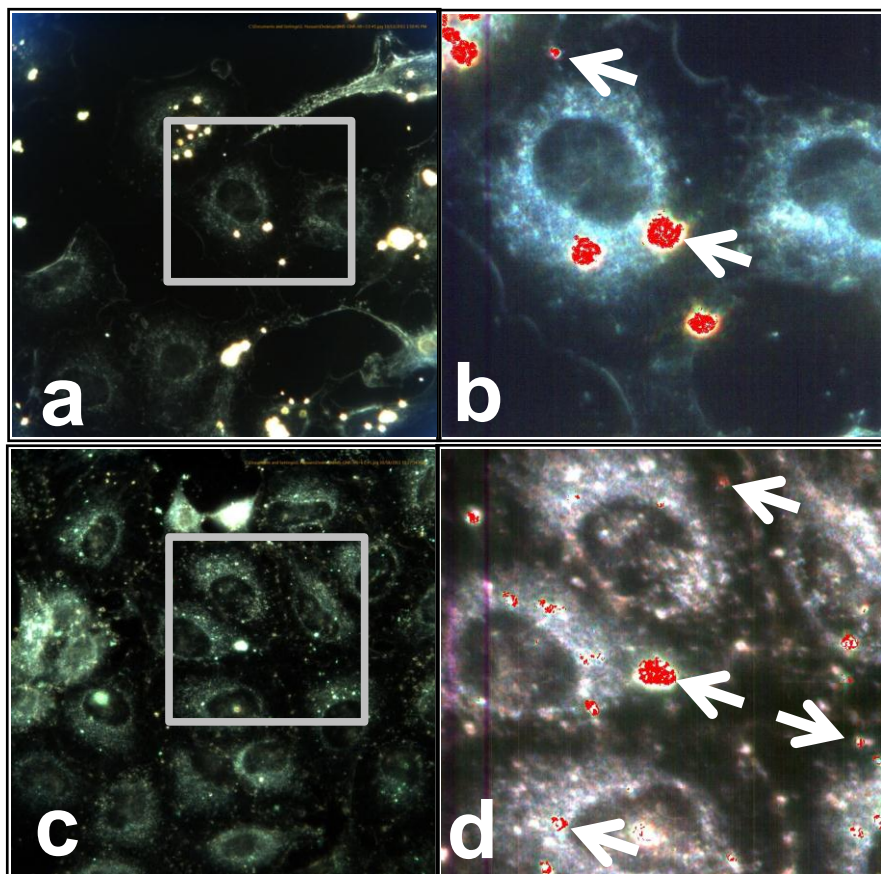


Fig. 5 In Vitro Identification of Gold Nanorods. **a** Darkfield images of A549 cells dosed with AR 2.5 GNRs. **b** Successful 2.5 AR GNR identification following HSI analysis as indicated with pixilation and arrows. **c** Darkfield images of A549 cells and AR 6.0 GNRs. **d** *In vitro* AR 6.0 identification as indicated with pixilation and arrows. Sections **b** and **d** are the areas located with the squares of images **a** and **c**, respectively.

The main difference seen was that AR 2.5 was primarily identified in large agglomerates, while AR 6.0 was tagged as both agglomerates and individual particles. We believe that this is due to the use of the longitudinal peak of AR 2.5 GNRs with HSI system, which was shown to contain a significant plasmon coupling effect in media. While numerous spectral profiles were used for

this identification process, it is extremely difficult to predict the spectral shift of GNRs resulting from plasmon coupling during agglomeration. On the contrary, with AR 6.0 a higher selectivity of individual particles *in vitro* was observed. The cause for this increased effectiveness is that for AR 6.0 the transverse resonance peak was used for sensing, which demonstrated a minimal spectral shift. As the spectral profiles displayed a more uniform appearance, it was considerably easier for the HSI system to align captured spectral profiles to that of an individual GNR particle as well as agglomerates.

4.0 CONCLUSIONS

Gold nanorods of two different aspect ratios (2.5 and 6.0) were successfully identified *in vitro* using a hyperspectral imaging system through their unique optical signatures (Figure 6). The observed shift in the GNR dependent spectral properties was due to plasmon coupling between particles following their aggregation, and was dependent on whether the transverse or longitudinal resonance peak was utilized for recognition. This study verified that the shift in longitudinal peaks was significantly greater than the transverse peaks, indicating that the transverse peak may be optimal for sensing applications. As such, it may be expedient to implement the utilization of transverse wavelengths for nano-based sensing or imaging application utilizing GNRs. Furthermore, we successfully demonstrated that the employment of HSI as a feasible technique for the tracking and identification of nanomaterials in an *in vitro* environment. This study also demonstrated that HSI technology is capable of overcoming the complication of plasmon coupling effects frequently seen with nanomaterials. However, the specificity of this methodology is directly linked to the observed degree of spectral shifting in cellular environments, an important fact to consider for the future utilization of HSI. In conclusion, this study successfully validated the emerging HSI technology as a viable technique to track and monitor GNR fate in a physiological environment, demonstrating the potential of this instrument to handle a more complex nano-shape imaging analysis.

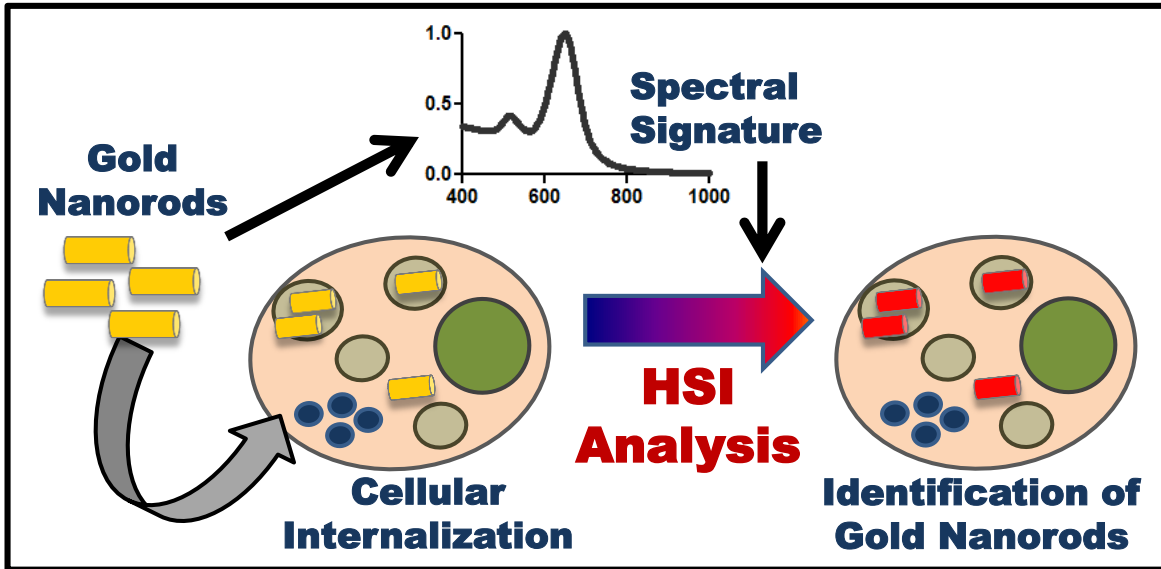


Fig. 6 Summary of HSI Technology and Work Performed. Gold nanorods were synthesized in house with either an aspect ratio of 2.5 or 6. During characterization, the unique spectral signature of these particles was obtained both in water and in growth media. An in vitro system was then exposed to both sets of nanorods, and the rods were selectively identified through their spectral signature using an advanced hyperspectral imaging (HSI) technology.

5.0 REFERENCES

1. Daniel MC, Astruc D (2004) Gold nanoparticles: assembly, supramolecular chemistry, quantum-size-related properties, and applications toward biology, catalysis, and nanotechnology. *Chem Rev* 104:293-346.
2. Panyala NR, Pena-Mendez EM, Havel J (2009) Gold and nano-gold in medicine: Overview, toxicology and perspectives. *J Appl Biomed* 7:75-91.
3. Wang Y, Xie X, Wang X, Ku G, Gill KL, O'Neal DP, Stoica G, Wang LV (2004) Photoacoustic tomography of a nanoshell contrast agent in the in vivo rat brain. *Nano Lett* 4:1689-1692.
4. Lewinski N, Colvin V, Drezek R (2008) Cytotoxicity of nanoparticles. *Small* 4:26-49.
5. Dreaden EC, Alkilany AM, Huang X, Murphy CJ, El-Sayed MA (2012) The golden age: Gold nanoparticles for biomedicine. *Chem. Soc Rev* 41:2740-2779.
6. Murphy CJ, Gole AM, Stone JW, Sisco PN, Alkilany AM, Goldsmith EC, Baxter SC (2008) Gold nanoparticles in biology: Beyond toxicity to cellular imaging. *Acc Chem Res* 41:1721-1730.
7. Goh D, Gong T, Dinish US, Maiti KK, Fu CY, Yong KT, Olivo M (2012) Pluronic triblock copolymer encapsulated gold nanorods as biocompatible localized plasmon resonance-enhanced scattering probes for dark-field imaging of cancer cells. *Plasmonics* 7:595-601.
8. Link S, El-Sayed MA (1999) Spectral properties and relaxation dynamics of surface plasmon electronic oscillations in gold and silver nanodots and nanorods. *J Phys Chem B* 103:8410-8426.
9. Garcia MA (2011) Surface plasmons in metallic nanoparticles: Fundamentals and applications. *J Phys D: Appl Phys* 44:283001.
10. Huang X, Neretina S, El-Sayed MA (2009) Gold nanorods: From synthesis and properties to biological and biomedical applications. *Adv Mat* 21:4880-4910.
11. Huang X, El-Sayed IH, Qian W, El-Sayed MA (2006) Cancer cell imaging and photothermal therapy in the near-infrared region by using gold nanorods. *J Am Chem Soc* 128:2115-2120.

12. Zhu J, Huang L, Zhao J, Wang Y, Zhao Y, Hao L, Lu Y (2005). Shape dependent resonance light scattering properties of gold nanorods. *Mat Sci Eng B* 121:199-203.
13. Tabor C, Haute DV, El-Sayed MA (2009). Effect of orientation on plasmonic coupling between gold nanorods. *ACS Nano* 3:3670-3678.
14. Kumar S, Harrison N, Richards-Kortum R, Sokolov K (2007). Plasmonic nanosensors for imaging intracellular biomarkers in live cells. *Nano Lett* 7:1338-1343.
15. Curry M, Crow J, Wax A (2008). Molecular imaging of epidermal growth factor receptor in live cells with refractive index sensitivity using dark-field microspectroscopy and immunotargeted nanoparticles. *J Biomed Opt* 13:014022.
16. Wax A, Sokolov K (2009). Molecular imaging and darkfield microspectroscopy of live cells using gold plasmonic nanoparticles. *Laser Photonics Rev* 3:146-158.
17. Aaron J, Travis K, Harrison N, Sokolov K. (2009). Dynamic imaging of molecular assemblies in live cells based on nanoparticle plasmon resonance coupling. *Nano Lett* 9:3612-3618.
18. Rocha A, Zho Y, Kundu S, Gonzalex JM, BradleighVinson S, Liang H (2011). In vivo observations of gold nanoparticles in the central nervous system of *Blaberus discoidalis*. *J Nanobiotechnology* 9:5.
19. Mukhopadhyay A, Grabinski C, Afrooz AR, Saleh NB, Hussain S (2012). Effect of gold nanosphere surface chemistry on protein adsorption and cell uptake in vitro. *Appl Biochem Biotechnol* 167:327-337.
20. Altinoğlu EI, Adair JH (2010). Near infrared imaging with nanoparticles. *WIREs Nanomed Nanobiotechnol* 2:461-477.
21. Jana NR, Gearheart LA, Obare SO, Johnson CJ, Edler KJ, Mann S, Murphy CJ (2002). Liquid crystalline assemblies of ordered gold nanorods. *J Mat Chem* 12:2909-2912.
22. Park K, Vaia RA (2008). Synthesis of complex Au/Ag nanorods by controlled overgrowth. *Adv Mat* 20:3882-3886.
23. Alkilany AM, Nagaria PK, Hexel CR, Shaw TJ, Murphy CJ, Wyatt MD (2009). Cellular uptake and cytotoxicity of gold nanorods: Molecular origin of cytotoxicity and surface effects. *Small* 5:701-708.

24. Link S, Mohamed MB, El-Sayed MA (1999). Simulation of the optical absorption spectra of gold nanorods as a function of their aspect ratio and the effect of medium dielectric constant. *J Phys Chem B* 103:3073-3077.
25. Sethi M, Joung G, Knecht MR (2009). Stability and electrostatic assembly of Au nanorods for use in biological assays. *Langmuir* 25:317-325.
26. Jain PK, Eustis S, El-Sayed MA (2006). Plasmon coupling in nanorod assemblies: Optical absorption, discrete dipole approximation simulation, and exciton-coupling model. *J Phys Chem B* 110:18243-18253.
27. Yu D, Ganta D, Dale E, Rosenberger AT, Wicksted JP, Kalkan AK (2012). Absorption properties of hybrid composites of gold nanorods and functionalized single-walled carbon nanotubes. *J Nanomaterials* 2012:154278.

LIST OF ABBREVIATIONS AND NOTATIONS

AR	Aspect Ratio
BDAC	Benzyldimethylammonium Chloride
CTAB	Cetyltrimethylammonium Bromide
GNRs	Gold Nanorods
HSI	Hyperspectral Imaging
NIR	Near Infrared
TEM	Transmission Electron Microscope
UV-VIS	Ultraviolet and Visible Absorption Spectroscopy